Clim. Past Discuss., 10, 3661–3688, 2014
www.clim-past-discuss.net/10/3661/2014/
doi:10.5194/cpd-10-3661-2014

Climate of the Past
Discussions
Open Access

Oxygen isotopic analyses of individual planktic foraminifera species: implications for seasonality in the western Arabian Sea

P. D. Naidu[1], **N. Niitsuma**[2], **and S. Naik**[1]

[1]CSIR – National Institute of Oceanography Dona Paula 403 004, Goa, India
[2]Institute of Geosciences, Shizuoka University, 836 Oya, Shizuoka 422-8529, Japan

Received: 13 August 2014 – Accepted: 25 August 2014 – Published: 1 September 2014

Correspondence to: P. D. Naidu (divakar@nio.org)

Published by Copernicus Publications on behalf of the European Geosciences Union.

Abstract

The variation of stable isotopes between individual shells of planktic foraminifera of a given species and size may provide short-term seasonal insight on Paleoceanography. In this context, oxygen isotope analyses of individual *Globigerinoides sacculifer* and *Neogloboquadrina dutertrei* were carried out from the Ocean Drilling Program Site 723A in the western Arabian Sea to unravel the seasonal changes for the last 22 kyr. δ^{18}O values of single shells of *G. sacculifer* range from of 0.54 to 2.09 ‰ at various depths in the core which cover a time span of the last 22 kyr. Maximum inter-shell δ^{18}O variability and high standard deviation is noticed from 20 to 10 kyr, whereas from 10 kyr onwards the inter shell δ^{18}O variability decreased. The individual contribution of sea surface temperature (SST) and sea surface salinity (SSS) on the inter shell δ^{18}O values of *G. sacculifer* were quantified. Maximum seasonal SST between 20 and 14 ka was caused due to weak summer monsoon upwelling and strong cold winter arid continental winds. Maximum SSS differences between 18 and 10 ka is attributed to the increase of net evaporation minus precipitation due to the shift of ITCZ further south. Overall, winter dominated SST signal in Greenland would be responsible to make a teleconnection between Indian monsoon and Greenland temperature. Thus the present study has wider implications in understanding wether the forcing mechanisms of tropical monsoon climate lies in high latitudes or in the tropics.

1 Introduction

Arabian Sea experiences the highest seasonal changes in terms of sea surface temperature, biological productivity, aeolion and fluvial terrigenious material supply predominantly driven by seasonal reversal of southwest (SW) and northeast (NE) monsoon winds. Extensive work has been carried out in understanding the monsoon variability on glacial and interglacial time scale (Prell, 1984; Anderson and Prell, 1993) and on millennial time scales (Sirocko et al., 1993; Naidu and Mamgren, 1996; Schulz et al., 1998). Studies have also been made to reconstruct the sea surface temperature (Rostek et al., 1997; Dahl, 2006; Saher et al., 2007; Rashid et al., 2007; Anand et al., 2008; Govil and Naidu, 2010), fluctuations of oxygen minimum zone (Reichart et al., 1993) and denitrification (Altabet et al., 1995). Previously, by using transfer functions and artificial neural network techniques on planktonic foraminiferal census data seasonal SST was reconstructed for February and August by CLIMAP (1981) and winter and summer SST by Naidu and Malmgren (2005). Although the Arabian Sea documents highest seasonal SST and SSS and seasonality is an important diagnostic of the climate system and also climate change mechanism, no efforts have been made to understand the seasonal SSS changes in the geological past. For the first time an attempt has been made to reconstruct seasonal SSS by using single shell analyses of planktonic foraminifer species *G. ruber* and *N. dutertrei* in order to understand the relationship between monsoon and seasonality over the last 22 kyr.

2 Strategy

Generally the isotopic analysis are conducted on 10 to 30 foraminiferal tests are combined into a single sample. Assemblage of individuals from which the shells were picked spans a large temporal range, both seasonal and annual, hence the single value obtained represents an average of environmental information present. Short-lived events such as episodic or seasonal changes, which were recorded by several individuals, could be masked by the averaged temperature signal. Therefore, the components of the short duration signal cannot be identified and interpreted meaningfully hence isotopic values of single shell foraminifera will be able to trace the seasonal and short-lived events through the time. In this connection, variation of stable isotope ratios between individual shells of planktonic foraminifera of a given species and size have been used to depict seasonal oceanographic changes in the Pacific (Killingley et al., 1981; Oba, 1990; Spero et al., 1990) Mediterranean (Tang and Stott, 1993) and Indian Ocean (Niitsuma et al. 1991; Ganssen et al., 2011). In this study we have used single shells of *G. sacculifer* and *N. dutertrei* for oxygen and carbon isotopes in order to document seasonal changes at the ODP Site 723A from the western Arabian Sea.

3 Oceanography

Circulation in the Arabian Sea is controlled by the seasonal reversal of the SW and NE monsoon winds caused by the alternate heating and cooling of the Tibet Plateau. During summer (June through September) strong southwesterly winds blow across the Arabian Sea, which causes offshore Ekman transport and intense upwelling along the Oman and Somalia margins and the southwest coast of India (Wyrtki, 1973). The upwelling process brings cold, nutrient-rich waters from few hundred meters depth into the surface and fuels the biological productivity in the euphotic zone and cools the sea surface temperature. Maximum sea surface temperature prevails during pre southwest monsoon and minimum during SW monsoon. Strikingly winter SST (NE monsoon) are slightly warmer than summer SST (SW monsoon) (Fig. 1). By contrast, salinity exhibit minimum contrast between SW and NE monsoons (Fig. 1). Thus upwelling process also creates an east to west temperature gradient in the Arabian Sea. During winter the northeasterly winds suppresses the upwelling and causes low biological productivity. Therefore, seasonal reversal of the wind direction and associated circulation pattern has a direct bearing on the biological productivity in the Arabian Sea (Kobanova, 1968) and the lithogenic and biogenic flux supply to the sediment (Nair et al., 1989). Thus, Arabian Sea experiences high seasonality in terms of temperature and productivity.

4 Material and methods

Ocean Drilling Program Site 723A is located in the region of intense upwelling and highest sedimentation rate along the Oman Margin in the Arabian Sea (Prell and Niitsuma, 1989) (Fig. 2). Chronology for the Site 723A is based on 13 AMS ^{14}C ages (Naidu and Malmgren, 2005) and covers the time span of the last 22 kyr (Table 1).

We have chosen *G. sacculifer* and *N. dutertrei* for single shell analyses because both these species live throughout the year in the Arabian Sea (Curry et al., 1992) and *G. sacculifer* lives in the mixed layer and *N. dutertrei* lives in the thermocline depth (Hemelben et al., 1989). Individual shells of *G. sacculifer* (without sac) and *N. dutertrei* with size ranging from 500 to 600 µm were put in a stainless-steel thimble. Few drops of methyl alcohol was dropped into the thimble, the individual tests were gently cracked by using a thin needle, and cleaned in a ultrasonic bath by viewing the cleaning process under binocular microscope. The cleaned individual carbonate test was reacted in saturated pyrophosphoric acid at 60°C in a vaccum system on-line to a MAT 250 Mass Spectrometer with ultra small sample gas inlet system. The isotopic composition of the evolved CO_2 gas is reported in δ notation as per mil (‰) deviations from PDB. Calibration was made through the standard carbonate NBS-20, assuming its oxygen and carbon isotopic composition versus PDB to be −4.18 and −1.07 ‰, respectively (Craig, 1957). The analytical precision, estimated from repeated analyses of un-roasted NBS-20 carbonate reacted under conditions identical to that of the foraminiferal samples was 0.02 ‰ for carbon 0.05 ‰ for oxygen.

The $\delta^{18}O_W$ is calculated by using the fallowing equation of Bemis et al. (1998):

$$\delta^{18}O_W(\text{V-SMOW}) = 0.27 + (T(^\circ C) - 16.5 + 4.8^{*}\delta^{18}O_{\text{calcite}}(\text{V} - \text{PDB}))/4.8 \tag{1}$$

Here summer and winter SST estimates based on Artificial Neural Network (ANN) (Naidu and Malmgren, 2005) were used to estimate the $\delta^{18}O_W$ from the extreme end values of individual δ^{18}Oc of *G. sacculifer*. Global ice volume values of Shackleton (2000) were subtracted from δ^{18}Ow values obtained from Eq. (1) to derive the local δ^{18}Ow variations which represents seasonal evaporation and precipitation in the region. δ^{18}Ow values were converted to salinity by using the equation $S = (\delta^{18}\text{Ow} + 15.2)/0.45$ given by Rostek et al. (1993). At each interval the SST and SSS difference between summer and winter are presented in Table 1. Due to the non-availability of thermocline SST, δ^{18}Ow values are not computed for the thermocline dwelling planktonic foraminifer species *N. dutertrei*. Standard deviations obtained from the individual species analyses of δ^{18}Oc of *G. sacculifer* and *N. dutertrei* are presented in Table 2.

5 Results

The δ^{18}O values of *G. sacculifer* show a high range (1 to 2 ‰) of inter shell variability between 20 and 10 ka and low variability (< 1 ‰) between 8 to 0.5 ka (Fig. 3). Inter shell variability of δ^{18}O values of *N. dutertrei* document highest range (> 1 ‰) from 17 to 10 ka and less range (< 1 ‰) from 22 to 19 and 8 to 0.5 ka (Fig. 4).

Difference between summer and winter SST was highest between 20 and 14 ka and the seasonal SSS difference was highest from 18 to 10 ka (Fig. 5). Both SST and SSS display lowest seasonal difference from 8 to 0.5 ka. Mean δ^{18}O of *G. sacculifer* display 1.5 ‰ shift between last glacial maximum (LGM) as compared to the core top values (Fig. 3). Similarly, mean δ^{18}Oc of *N. dutertrei* shows 1.5 ‰ shift between LGM and Holocene (Fig. 4).

6 Discussion

The variability of isotopic ratios between shells of the individual specimens of same species at the same stratigraphic level must be due to following four causes as stated by (Killingly et al., 1981): (1) mixing of individuals from older and younger geological periods by organisms on the sea floor (i.e bioturbation); (2) seasonal and longer-term variations in the temperature and isotopic composition of the sea water within which the shells grew; (3) variations in depth of calcification; and (4) variations in metabolic or vital effects. The ODP Site 723A is located in the oxygen minimum zone (OMZ) and this area receives high sedimentation (35 to 60 cm ka^{-1}) (Naidu and Malmgren, 1995) therefore bioturbation effect on the inter shell variations of δ^{18}O may be negligible. Also the effect of stable isotope variation in depth of calcification would not affect our results because the size range > 500 µm will not influence ontogenic effect on the oxygen and carbon isotopic ratios in the Indian Ocean (P. D. Naidu, manuscript in preparation, 2014). The mixing model shows that the observed inter shell changes of oxygen isotope values are not due to the mixing through bioturbation. Therefore, we believe that the individual shell δ^{18}O changes would reflect the seasonal isotopic changes of water in which the foraminifera grew and thus inter shell δ^{18}O variability are interpreted as seasonal temperature and salinity changes at the core location. Thus, single shell analysis has particular advantage in depicting seasonal changes and the short-lived anomalous conditions in ocean history and these changes should appear as distinct modes in the distribution of isotopic values at a given time.

It is apparently clear that inter shell δ^{18}O variability was higher during the last glacial period than in the Holocene, but strikingly highest variability was documented during deglaciation. The inter shell δ^{18}Oc variability at this site is attributed to the seasonal temperature and salinity variations. This site is located in the intense upwelling zone of the Arabian Sea; most of the δ^{18}O changes documented here should reflect the temperature variations modulated by the upwelling through time in the western Arabian Sea. Not only in the present day but also in the geological past the western Arabian Sea SST is controlled by the upwelling process (Naidu and Malmgren., 2005; Shital et al., 2011).

6.1 Seasonal SST changes

Observed maximum temperature contrast between 20 and 14 kyr is primarily attributable to the variation of upwelling intensity at this site. Weak upwelling strength from 20 to 14 kyrs (Naidu and Malmgren, 1996; Overpeck et al., 1996) would increase the summer SST in this region, whereas the strong NE monsoon continental winds which were cool and dry might have lowered the winter SST. In addition to weak upwelling, during last glacial period, there is an evidence for dustier conditions (Thomson et al., 1997) so perhaps increased aerosol levels in the atmosphere which might further decreases the winter SST in this region. Thus, weak upwelling, strong cold continental winds and more aerosol concentrations during winters caused maximum seasonal

SST in the western Arabian Sea during the last glacial period. Similarly, upwelling was intense during the Holocene (Naidu and Malmgren, 1996; Overpeck et al., 1996), which lowers the SST during summer, and winter NE monsoon winds were weak during Holocene (Govil and Naidu, 2011), therefore minimum seasonal SST contrasts observed at this site. The difference in solar insolation changes between summer and winter season at 30° N was maximum from 12 to 6 kyr (Fig. 5), which does not coincide with the maximum seasonal SST difference at this site further reveals that SST changes at this location were governed by the seasonal upwelling process rather than solar insolation. Similarly greater range in upwelling seasonality during Holocene than in the last glacial period is documented based on the oxygen isotopes values obtained on single specimens of *G. ruber* and *G. bulloides* in a Core 905 from Off-Somalia (Ganssen et al., 2012). The seasonal ranges of temperature and salinity, we presented in this paper are summer and winter seasons. Whereas Ganssen et al. (2012) SST ranges represents upwelling and non-upwelling seasons hence these two data sets express different seasonal temperatures ranges during Holocene and last glacial period. Alike to present study, seasonal temperatures was greater during LGM than in Holocene in the north Pacific (Lee et al., 2003) and in the western Mediterranean (Fergusson et al., 2011).

6.2 Seasonal sea surface salinity changes

After removing the temperature and global ice volume components from δ^{18}Oc, δ^{18}Ow is expected to reflect the sea surface salinity which depends on the regional evaporation and precipitation in the western Arabian Sea. In general high SSS prevails in the Arabian Sea during winter months due to high evaporation and less precipitation, on the other hand, the upwelling process and overhead precipitation during SW monsoon lowers SSS in the western Arabian Sea (Levitus et al., 1994). Our reconstruction of seasonal SSS over last 22 kyr reveals that the highest seasonal SSS variations occurred between 10 and 18 ka (Fig. 6). More evaporation during glacial winters and least evaporation and minimum overhead precipitation during glacial summers have caused high seasonal SSS contrast from 10 to 18 ka in the western Arabian Sea. Overall, SW monsoon was weaker during the last glacial period (Prell, 1984; Naidu and Malmgren, 1996; Overpeck et al., 1996), therefore, the observed high seasonal SSS cannot be explained by the rainfall associated with SW monsoon. We suggest that most probable candidate for driving the observed SSS contrast during the last glaciation is the changes of evaporation between summer and winter caused by the seasonal migration of ITCZ in the Indian Ocean. Seasonal migration of ITCZ was minimal during the last glacial period (Denton et al., 2005) and southward shift of ITCZ during last glacial period would increase the net evaporation minus precipitation during winter in the Oman Margin which would cause high SSS as evident from the present data set (Fig. 5). The enhanced evaporation during winter not only cools the surface waters but also increases the upper-layer salinity. Whereas during summer evaporation was reduced due to weak summer monsoon winds which lower the SSS. Thus the seasonal migration of ITCZ would cause major changes in evaporation pattern between summer and winter in the western Arabian Sea. Conversely seasonal migration of ITCZ during the last glacial maximum (21 ka) was minimal and evaporation was more or less same between summer and winter causing minimum seasonal SSS difference. Mean position of the ITCZ moved to north during Holocene which might have reduced the winter evaporation and increase the summer upwelling and rainfall causing minimum seasonal SSS from 9 to 0 kyr.

6.3 Seasonal SST and SSS contrast and Inter Tropical Convergence Zone (ITCZ)

Seasonality is a key diagnostic variable of the climate system and mechanism of climate change (Guilderson et al., 2001). Precession of the Equinox changes the Earth–Sun distance which determines the amount of solar radiation received by the earth in a particular season. In consequence, precession cycle of the Earth's orbit determines the strength of monsoon winds and variation in seasonality and ITCZ position in the Indian Ocean (Clemens et al., 2003). During the Boreal Summer, the ITCZ migrates northward across the Indian Ocean and the Indian subcontinent, bringing its summer monsoon rainfall. In late Fall the ITCZ retreats southward decreasing the rainfall. Thus, variations in rainfall on inter annual and longer time scale are controlled by the variation in moisture derived from convective activity of the ITCZ in the Indian Ocean. The δ^{18}O record of speleotherm calcite from Qunf Cave provided good evidence on changes in precipitation rates and shown that an increase in precipitation and the δ^{18}O values become more positive when the ITCZ is overhead, whereas the ITCZ moves south, precipitation decreases and the δ^{18}O values become more positive (Fleitmann et al., 2003). Therefore, seasonal migration of the ITCZ position determines the amount of precipitation over the Indian subcontinent and the position of ITCZ has shifted depending on the seasonal variability in the past. Changes in the position of ITCZ during the Holocene are also recorded in the sedimentary record of the Cariaco Basin off the coast of northern Venezuela (Haug et al., 2001). Comparison of annual, summer and winter SST variations at ODP Site 723A reveals that winter SST exhibit greater magnitude of variations than summer SST during the last glacial period indicating the influence of winter SST in pushing the ITCZ southward.

Thermocline dwelling species *N. dutertrei* document maximum inter shell δ^{18}Oc values from 14 to 12 ka revealing that thermocline depth was shallow during the deglaciation which replicates the hydrography of surface waters as documented in *G. sacculifer.* Further, *G. sacculifer* and *N. dutertrei* show same mean δ^{18}O values during 9 ka (Figs. 3 and 4) suggesting a shallowing of thermohaline depth due to intense upwelling in the western Arabian Sea.

6.4 Greenland and monsoon teleconnection through seasonality

Monsoon reconstructions based on proxies such as *Globigerina bulloides* abundances (Gupta et al., 2003), total organic carbon record (Schulz et al., 1998) from marine sediment cores from the Arabian Sea and oxygen isotopic ratios of speleotherms from Oman (Fleitmann et al., 2003) and China (Wang et al., 2001) have demonstrated that abrupt changes in monsoon intensity coincide with temperature changes indicated in the Greenland GISP2 ice core record. In the same way, millennial-scale paleoclimate records of the last glaciation show striking similarities across a huge area of the planet from Greenland to eastern Asia (Denton et al., 2005). These similarities include not only the number and spacing, but also the relative magnitudes of stades and interstades in monsoon records, for example δ^{15}N (Altabet et al., 2003) and productivity records (Singh et al., 2011) from the Arabian Sea. Such similarities, in millennial scale climate records between Greenland and in the tropics imply that a common forcing mechanism transmits the paleoclimate signal from Greenland to Asia.

Previously it has been speculated by Denton et al. (2005) that winter-dominated seasonality switches of North Atlantic and Greenland might be driving the millennial-scale oscillations of the Atlantic ITCZ (Hughen et al., 1996), the Asian monsoon (Schulz et al., 1999; Wang et al., 2001) and surface and intermediate waters of eastern North Pacific (Hendy and Kennett, 1999). But it is not known whether winter-dominated temperature in Greenland influence the tropical winter temperature, in this context our data of individual shell δ^{18}O of *G. ruber* and *N. duterteri* lends support that the winter temperature in the Arabian Sea also show strong seasonality (Fig. 7). Therefore, it is proposed here that winter seasonality was the common forcing linkage between Greenland-European temperatures, the Atlantic ITCZ and Asian monsoons. The consequences of changes in seasonality in Greenland propagated millennial scale abrupt climate change in the northern hemisphere and into the tropics (Denton et al., 2005). Further, a tenfold increase of dust during stadials in Greenland (Mayewski et al., 1997) which is derived from the deserts of western China (Biscaye et al., 1997) provides an additional atmospheric link not only to the summer monsoon but also to the winter monsoons.

In Greenland the switches in mean annual temperature were dominated by large winter changes, and thus temperatures during winter control the seasonality in Greenland (Denton et al., 2005). Existence of identical Greenland and monsoon signals at millennial scale particularly between 10 and 60 ka (Schulz et al., 1998; Wang et al., 2001) and maximum seasonal SST difference during last glaciation as evident from the present study would reveal that winter dominated seasonality was common in both the regions.

Severe Greenland winters would reduce the winter temperature over Eurasia leading to heavy snow fall in the western Himalyas result in weakening or collapse of Indian summer monsoon (Blanford, 1884) and thus large Eurasian snowpack would cause large scale regional climate change. Recent studies have also emphasized the relationship between spatial pattern of snow cover in Tibet and summer monsoon (Zhao and Moore, 2004). Late-lasting winter snowfall carries over well into the summer, thus slowing summer warming of the Asian land mass and reducing the land-sea temperature contrast that is a primary driver of the summer monsoon. Modelling studies also confirm that a link between the Eurasian snow cover during winters to follow on summer monsoons (Barnett et al., 1988), which offers a physical mechanism whereby long-lasting winter snow cover on the Eurasian land mass during glacial stades would link a weak Asian summer monsoon with cold Greenland and European winter temperatures.

Abrupt millennial scale fluctuations were not present during Holocene in the Greenland temperature records but Indian and Asian monsoon records document greater magnitude fluctuations during Holocene (Wang et al., 2001; Gupta et al., 2003; Fleitman et al., 2003; Govil and Naidu, 2010). This reveals that minimum seasonal shifts between winter and summer temperatures in the Greenland would unable to propagate the temperature signal to the monsoon influenced regions causing asynchrony between Greenland and Asian Monsoon records during Holocene. Thus, Holocene variability in the Indian and Asian monsoon records is perhaps forced by the solar insolation changes rather than the Greenland temperatures.

Previously two mechanisms were proposed to explain inter decadal and centennial scale fluctuations of the Indian monsoon rainfall: A tropical teleconnection mechanism through ENSO involving shift of Walker Circulation influencing the regional monsoon Hadley Circulation (Krishnamurthy and Goswami, 2000; Sirocko et al., 1996). The other is an extratropical teleconnection mechanism in which a positive Atlantic Multidecadal Oscillation produces stronger monsoon by producing trophosphere temperature anomaly over Eurasia (Goswami et al., 2005). In principle, winter dominated temperature in Greenland would influence both Atlantic Multidecadal Oscillations and

ITCZ position in the tropics providing a common forcing mechanism in driving the coherent millennial scale abrupt climate shifts in the tropics.

7 Conclusions

Individual shells of planktonic foraminiferal species *G. sacculifer* and *N. dutertrei* were analyzed for oxygen isotopes at the ODP Site 723A, which provides seasonally resolved SST and SSS over last 22 kyr in the western Arabian Sea. Inter shell δ^{18}O values of *G. sacculifer* exhibit higher standard deviation during the last glacial period than in Holocene, driven by maximum seasonal SST and SSS changes in the western Arabian Sea. *N. dutertrei* shows maximum inter shell δ^{18}O variability during deglaciation period reflecting greater thermocline seasonality associated with deglaciation in the western Arabian Sea.

Maximum seasonality of SST during the last glacial period was caused due to greater winter cooling and reduced summer upwelling, while minimum SST seasonality during the Holocene was due to increased summer upwelling and reduced winter cooling. Highest SSS seasonality during the last glacial period was caused by the increase of winter evaporation and reduced monsoon rainfall, whereas during Holocene increased rainfall and reduced evaporation resulted in minimum SSS. Both evaporation and precipitation process are coupled with the seasonal migration of ITCZ in the western Arabian Sea.

Seasonality appears to be common link between Greenland temperatures and the various millennial scale climate records of the tropics in general and Indian and Asian Monsoon records in particular. Thus, both ITCZ shifts and propagation of Greenland temperature signal to other parts in the northern hemisphere perhaps depends on the seasonality.

Acknowledgements. We thank Japan Society for the Promotion of Higher Studies (JSPS) for providing financial support.

References

Altabet, M. A., Francois, D., Murray, W., and Prell, W. L.: Climate-related variations in denitrification in the Arabian Sea from $^{15}N/^{14}N$ ratios, Nature, 373, 506–509, 1995.

Anand, P., Kroon, D., Singh, A. D., Ganeshram, R. S., Ganssen, G., and Elderfield, H.: Coupled sea surface temperature–seawater $\delta^{18}O$ reconstructions in the Arabian Sea at the millennial scale for the last 35 ka, Paleoceanography., 23, PA4207, doi:10.1029/2007PA001564, 2008.

Anderson, D. M. and Prell, W. L.: A 300 kyr record of upwelling off Oman during the late Quaternary: evidence of the Asian southwest monsoon, Paleoceanography, 8, 193–208, 1993.

Barnett, T., Dumenil, L., Schlese, U., and Roeckner, E.: The effect of Euasian snow cover on global climate, Science, 239, 504–507, 1988.

Bemis, B. E., Spero, H. J., Bijma, J., and Lea, D. W.: Reevaluation of the oxygen isoto-pic composition of planktonic foraminifera: Experimental results and revised paleotemperature equations, Paleoceanography, 13, 150–160, doi:10.1029/98PA00070, 1998.

Biscaye, E., Grousset, F. E., Revel, M., Van der Gaast, S., Zielinski, G. A., Vaars, A. G., and Kukla, G.: Asian provenance of glacial dust (stage 2) in the Greeland Ice Sheet Project 2 Ice Core, Summit, Greenland. J. Geophys. Res., 102, 26765–26781, 1997.

Blanford, H. F.: On the connection of the Himalayan snowfall with dry winds and seasons of drought in India, P. Roy. Soc. London, 37, 3–22, 1884.

Clemens, S. C. and Prell, W. L.: A 350 000 year summer monsoon multi-proxy stack from the Owen Ridge, Northern Arabian Sea, Mar. Geol., 201, 35–51, 2003.

CLIMAP Project Members: Seasonal Reconstruction of the Earth' Surface at the Last Glacial Maximum, Map MC 36, Geol. Soc. Am., Boulder, Colorado, 1981.

Curry, W. B., Ostermann, D. R., Guptha, M. V. S., and Ittekkot, V.: Foraminiferal production and monsoonal upwelling in the Arabian Sea: Evidence from sediment traps, in: Upwelling Systems: Evolution Since the Early Miocene, edited by: Summerhayes, C. P., Prell, W. L., and Emeis, K. C., Geol. Soc. Spec. Publ. London, 64, 93–106, 1992.

Dahl, A. K. and Oppo, D. W.: Sea surface temperature pattern reconstructions in the Arabian Sea, Paleoceanography, 21, PA1014, doi:10.1029/2005PA001162, 2006.

Denton, G. H., Alley, R. B., Comer, G. C., and Broecker, W. S.: The role of seasonality in abrupt climate change, Quat. Sci. Rev., 24, 1159–1182, 2005.

Fairbanks, R. G.: A 17 000 year glacio-eustatic sea level record: influence of glacial melting rates on the Younger Dryas event and deep-ocean circulation, Nature, 342, 637–642, 1989.

Ferguson, J. E., Henderson, G. M., Fa, D. A., Finlayson, J. C., and Charnley, N. R.: 2011. Increased seasonality in the western Mediterranean during the last glacial from limpet shell geochemistry, Earth Planet. Sci. Lett., 308, 325–333, 2011.

Fleitmann, D., Burns, S. J., Mudelsee, M., Neff, U., Kramers, J., Mangini, A., and Matter, A.: Holocene forcing of the Indian monsoon recorded in a stalagmite from Southern Oman, Science, 300, 1737–1739, 2003.

Ganssen, G. M., Peeters, F. J. C., Metcalfe, B., Anand, P., Jung, S. J. A., Kroon, D., and Brummer, G. J. A.: Quantifying sea surface temperature ranges of the Arabian Sea for the past 20 000 years, Clim. Past, 7, 1337–1349, 2011, http://www.clim-past.net/7/1337/2011/.

Goswami, B. N. and Xavier, P. K.: ENSO control on the south Asian Monsoon through the length of the rainy season, Geophys. Res. Lett., 32, L18717, doi:10.1029/2005 GL023216, 2005.

Goswami, B. N, Madhusoodana, M. S., Neema, C. P., and Sengupta, D.: A physical mechanism for North Atlantic SST influence on the Indian Summer Monsoon, Geophys. Res. Lett., 33, L02706, doi:10.1029/2005 GL 024803, 2006.

Govil, P. and Naidu, P D.: Evaporation-precipitation changes in the eastern Arabian Sea for the last 68ka: Implications on monsoon variability, Paleoceanography, 25, PA1210, doi:10.1029/2008PA001687, 2010.

Guilderson, T. P., Fairbanks, R. G, and Rubenstone, J. L.: Tropical Atlantic coral oxygen isotopes: glacial-interglacial sea surface temperature and climate change, Mar. Geol., 172, 75–89, 2001.

Gupta, A. K., Anderson, D. M., and Overpeck, J. T.: Abrupt changes in the Asian southwest monsoon during the Holocene and their links to the North Atlantic Ocean, Nature, 421, 354–356, 2003.

Haug, G. H., Hughen, K. A., Sigman, D. M., Peterson, L. C., and Rohl, U.: Southward Migration of the Intertropical Convergence Zone through the Holocene, Science, 293, 1304–1306, 2001.

Hemleben, Ch, Spindler, M., and Anderson, O. R.: Modern Planktonic Foraminifera, Springer Verlag, Berlin, 363 pp., 1989.

Hendy, I. and Kennet, J.: Latest Quaternary North Pacific surface water responses imply atmosphere-driven climate instability, Geology, 27, 291–294, 1999.

Hughen, K. A., Overpeck, J. T., Peterson, L. C., and Trumbore, S.: Rapid climate changes in the tropical Atlantic region during the last deglaciation, Nature, 380, 51–54, 1996.

Killingley, J. S., Johnson, R. F., and Berger, W. H.: Oxygen and carbon isotopes of Individual shells of planktonic foraminifera from Ontong-Java Plateau, Equatorial Pacific, Palaeogeogr. Palaeoclimatol. Paleoecol., 33, 193–204, 1981.

Krishnamurthy, V. and Goswami, B. N.: Indian monsoon-ENSO relationship on inter decadal time scale, J. Climate, 13, 579–595, 2000.

Lee, K. E. and Park, Y. G.: Seasonal changes in sea surface temperature of the subtropical north Pacific during the last glaciation, Geosci. J., 7, 129–133, 2003.

Levitus, S., Burgett, R., and Boyer, T. P.: World Ocean Atlas 1994, Salinity, NOAA Atlas NESDIS 3, US Department of Commerce, Washington, DC, 99 pp., 1994.

Manabe, S. and Stouffer, R. J.: Coupled ocean-atmosphere model response to freshwater input: comparison to Younger Dryas Event, Paleoceanography, 12, 321–336, 1997.

Mayewski, A., Meeker, L. D., Twickler, M. S., Whitlow, S., Yang, Q., Lyons, W. B, and Prentice, M.: Major features and forcing of high-latitude northern hemisphere atmospheric circulation using a 110 000-year long glaciochemical series, J. Geophys. Res., 102, 26345–26366, 1997.

Naidu, P. D. and Malmgren, B. A.: A high-resolution record of late Quaternary upwelling along the Oman Margin, Arabian Sea based on planktonic foraminifera, Paleoceanography, 11, 129–140, 1996.

Naidu, P. D. and Malmgren, B. A.: Seasonal Sea Surface Temperature Contrast Between the Holocene and Last Glacial Period in the Western Arabian Sea (ODP Site 723A): Modulated by Monsoon Upwelling, Paleoceanography, 20, PA1004, doi:10.1029/2004PA001078, 2005.

Nair, R. R., Ittekkot, V., Manganani, S. J., Ramaswamy, V., Haake, B., Degens, E. T., Desai, B. N., and Honjo, S.: Increased particle flux to the deep ocean related to monsoons, Nature, 338, 749–751, 1989.

Niitsuma, N., Oba, T., and Okada, M.: Oxygen and carbon isotope stratigraphy at Site 723, Oman Margin, Proc. Ocean Drill. Prog. Sci. Results, 117, 321–341, 1991.

Oba, T.: Paleoceanographic Information Obtained by the Isotopic Measurement of Individual Foraminiferal Specimens, Proc. First Int'l. Conf. Asian Mar. Geol., Shanghai, 169–180, 1990.

Overpeck, J. T., Anderson, D. M., Trumbore, S., and Prell, W. L.: The southwest Indian monsoon over the last 18,000 years, Clim. Dyn., 12, 213–225, 1996.

Prell, W. L.: Variation of monsoonal upwelling: a response to changing solar radiation, in: Climatic Processes and Climate sensitivity, edited by: Hansen, J. E., and Takahashi, T., A. G. U., Maurice Ewing Ser., 5, 48–57, 1984.

Prell, W. L., and Niitsuma, N.: Site 723, Proc. Ocean Drill. Prog. Initial Rep., 117, 319-384, 1989.

Rashid, H., Flower, B. P., Poore, R.Z., and Quinn, T. M.: A ∼25 ka Indian Ocean monsoon variability record from the Andaman Sea, Quat. Sci. Rev., 26, 2586–2597, 2007.

Reichart, G. J., Lourens, L. J., and Zachariasse, W. J.: Temporal variability in the northern Arabian Sea Oxygen Minimum Zone (OMZ) during the last 225 000 years, Paleoceanography, 13, 607–621, 1998.

Rostek, F., Ruhland, G., Bassinot, F. C., Muller, P. J., Labeyrie, L. D, Lancelot, Y., and Bard, E.: Reconstructing sea surface temperature and salinity using δ18O and alkenone records, Nature, 364, 319–321, 1993.

Saher, M. H., Jung, S. J. A., Elderfield, H., Greaves, M. J., and Kroon, D.: Sea surface temperatures of the western Arabian Sea during the last deglaciation, Paleoceanography, 22, PA2208, doi:10.1029/2006PA001292, 2007.

Schulz, H. S, Von Rod, U., and Erlenkeuser, H.: Correlation between Arabian Sea and Greenland climate oscillations of the past 110 000 years, Nature, 393, 54–57, 1998.

Shackleton, N. J.: A 100 000 year ice-age cycle identified and found to lag temperature, carbon-dioxide, and orbital eccentricity, Science, 289, 1897–1902, 2000.

Shital, G., Naidu, P. D., and Malmgren, B. A.: Sea Surface Temperature Changes during May and August in the western Arabian Sea over the last 22 ka: Implications on shifting of upwelling season, Mar. Micropaleontol., 78, 25–29, 2011.

Singh, A. D., Jung, S. J. A., Darling, K., Ganeshram, R., Ivanochko, T., and Kroon, D.: Productivity collapses in the Arabian Sea during glacial cold phases, Paleoceanography, 26, PA3210, doi:10.1029/2009PA001923, 2011.

Sirocko, F., Garbe-Schonberg, D., McIntyre, A., and Molfino, B.: Teleconnection between the subtropical monsoons and high latitude climates during the last deglaciation, Science, 272, 526–529, 1996.

Spero, H. J. and Williams, D. F.: Evidence for seasonal low-salinity surface waters in the Gulf of Mexico over the last 16 000 years, Paleoceanography, 5, 963–975, 1990.

Tang, C. M. and Stott, L. D.: Seasonal salinity changes during Mediterranean sapropel deposition 9000 years BP: Evidence from isotopic analyses of individual planktonic foraminifera, Paleoceanography, 8, 473-493, 1993.

Thompson, L. G., Davis, H. E., Henderson, K. A., Mosley-thompson, E., Lin, P. N., Beer, J., Synal, H. A., Cole-Doi, J., and Bolzan, H. F.: Tropical climate instability: the last glacial cycle from a Qinhai Tibetan Ice Core, Science, 276, 1821–1825, 1997.

Wang, Y. J., Cheng, H., Edwards, R. L., An, Z. S., Wu, J. Y., Shen, C. C., and Dorale, J. A.: A high-resolution absolute-dated late Pleistocene monsoon record from Hulu Cave, China, Science, 294, 2345–2348, 2001.

Wyrtki, K.: Physical oceanography of the Indian Ocean, Vol. 3 of Ecological studies: analysis and synthesis, in: Biology of the Indian Ocean, edited by: Zeischel, B. and Gerlach, S. A., London: Chapman and Hall Ltd., 18–36, 1973.

Zhao, H. and Moore, G. W. K.: On the relationship between Tibetan snow cover, the Tibetan plateau monsoon and the Indian summer monsoon, Geophys. Res. Lett., 31, L14204, doi:10.1029/2004 GL020040, 2004.

Table 1. AMS ^{14}C dates used for establishing the chronology for ODP Site 723A 545 Naidu and Malmgren (2005).

S. No.	Depth (cm)	^{14}C Age	Calendar Years BP
1	3	950	280
2	16	1680	1005
3	39	2010	1330
4	64	2760	2254
5	96	3890	3587
6	121	4670	4622
7	154	6070	6276
8	186	7700	7938
9	218	8110	8359
10	274	9510	9854
11	316	10 500	10,877
12	520	15 920	18 200
13	740	19 130	22 260

Table 2. Winter and summer SST and salinity and their differences at the ODP Site 723A. Significant differences are shown in bold letters.

Age (ka)	Maximum SST	Minimum SST	Difference in SST	Winter salinity	Summer salinity	Difference in salinity
0.50	25.1	24.7	0.4	35.6	34.1	1.5
2.07	26.5	26.4	0.1	35.9	33.7	2.2
6.59	26.6	26.2	0.4	36.4	34.7	1.7
8.41	26.8	26.6	0.2	36.2	34.9	1.3
10.24	27	26.3	0.7	38.4	35	**3.4**
12.06	26.1	25.3	0.8	37	33.8	**3.2**
14.25	25.8	23.1	**2.7**	36.6	33.2	**3.4**
17.81	25.9	24.4	**1.5**	36.2	32.8	**3.4**
19.12	25	22.4	**2.6**	36.3	34.3	**2**
20.58	25.2	23	**2.2**	35.8	34.5	1.3
22.26	24.6	24.2	0.4	36.8	33.5	**3.3**

Table 3. Standard deviation values of *G. sacculifer* and *N. dutertrei* derived on the individual shell analyses of $\delta^{18}O$ at the ODP site 723A. Significant standard deviations are shown in bold letters.

Age (ka)	*G. sacculifer* $\delta^{18}O$ Standard deviation	*N. dutertrei* $\delta^{18}O$ Standard deviation
0.50	0.22	0.37
2.07	0.24	0.27
6.59	0.21	0.30
8.41	0.21	0.21
10.24	**0.54**	**0.44**
12.06	**0.51**	**0.53**
14.25	**0.7**	**0.47**
17.81	**0.53**	0.34
19.12	**0.45**	0.13
20.58	0.37	0.28
22.26	**0.45**	0.20

Title Page
Abstract Introduction
Conclusions References
Tables Figures
◂◂ ▸▸
◂ ▸
Back Close
Full Screen / Esc
Printer-friendly Version
Interactive Discussion

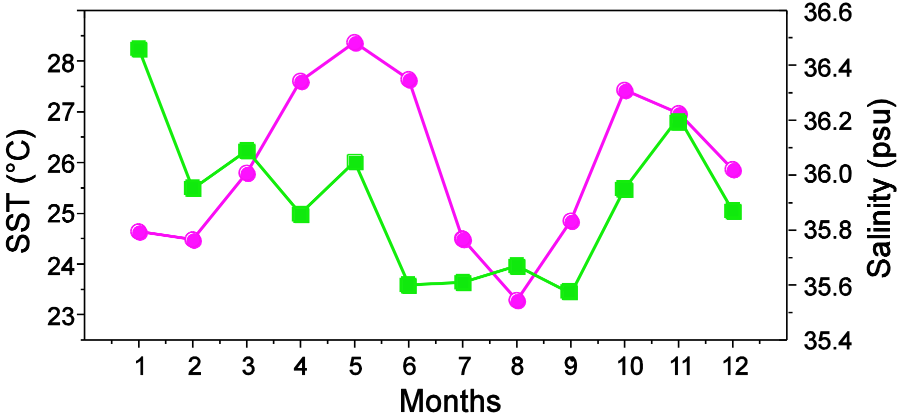

Figure 1. Variations of Sea surface temperature (violet color) and salinity (green color) at the location of ODP Site 723A in the western Arabian Sea (Levitus et al., 1994). Lowest sea surface temperature values during July, August and September caused by SW monsoon upwelling. More evaporation during winter months results in high sea surface salinity during NE monsoon.

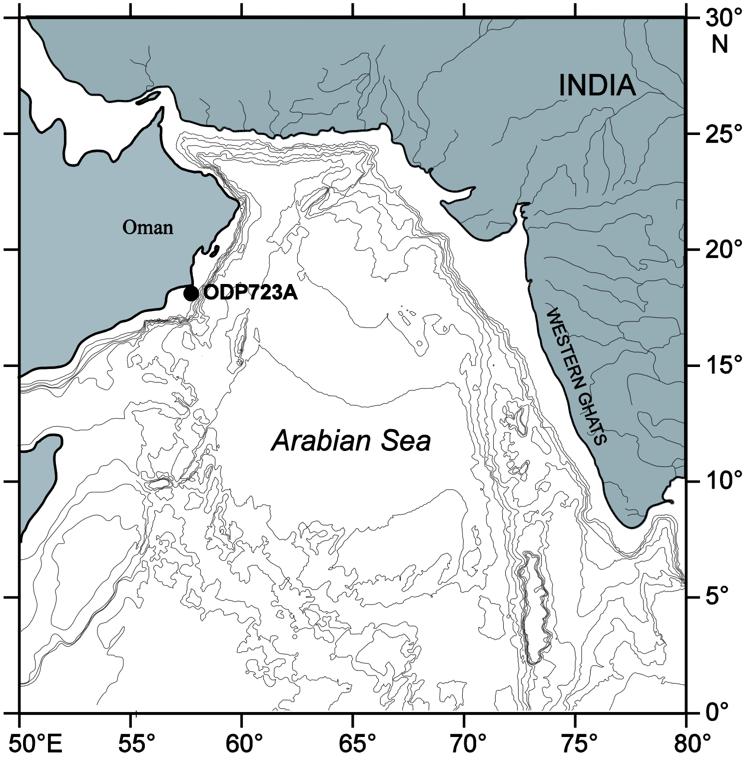

Figure 2. Location of ODP Site 723A in the western Arabian Sea.

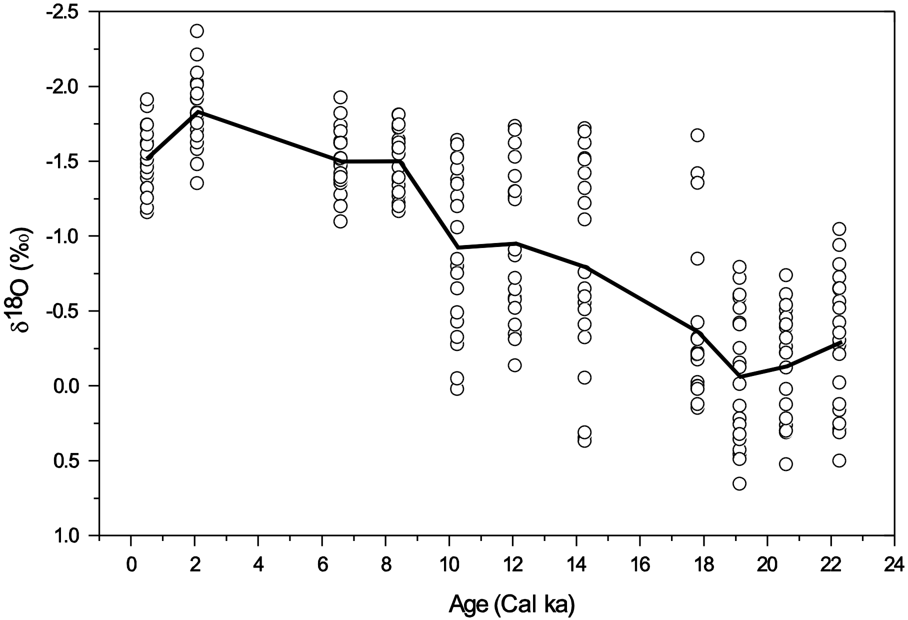

Figure 3. δ^{18}O values of individual *G. sacculifer* from the selected intervals, the line connects means value in each interval.

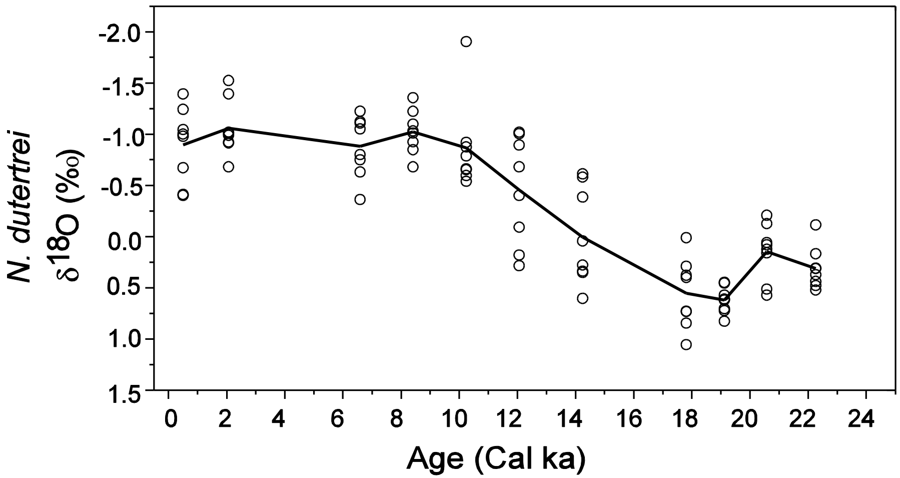

Figure 4. $\delta^{18}O$ values of individual *N. dutertrei* from the selected intervals, the line connects means value in each interval.

Title Page
Abstract
Introduction
Conclusions
References
Tables
Figures
◀
▶
Back
Close
Full Screen / Esc
Printer-friendly Version
Interactive Discussion

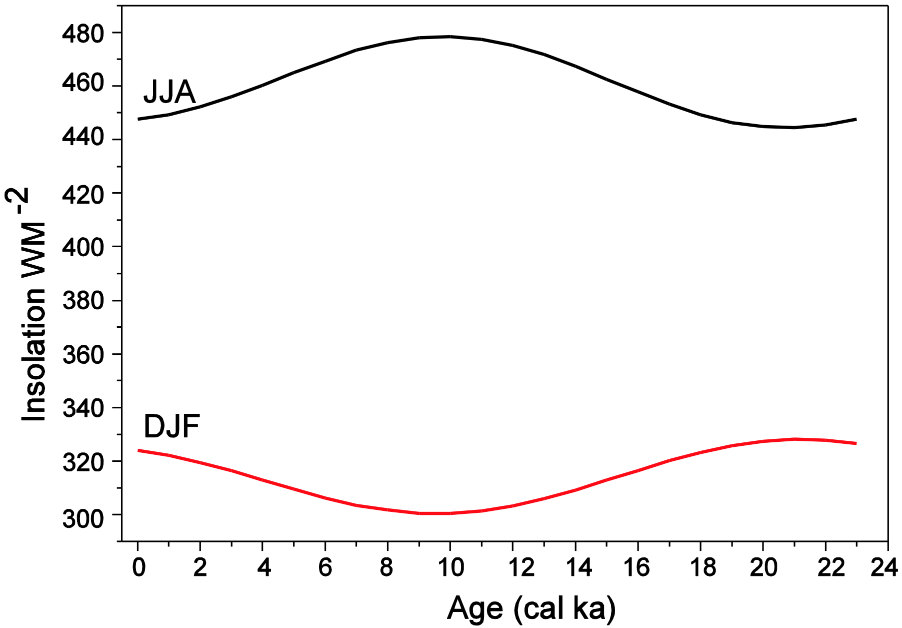

Figure 5. Solar insolation changes during June, July, August (JJA) and December, January, February (DJF) at 23° N latitude.

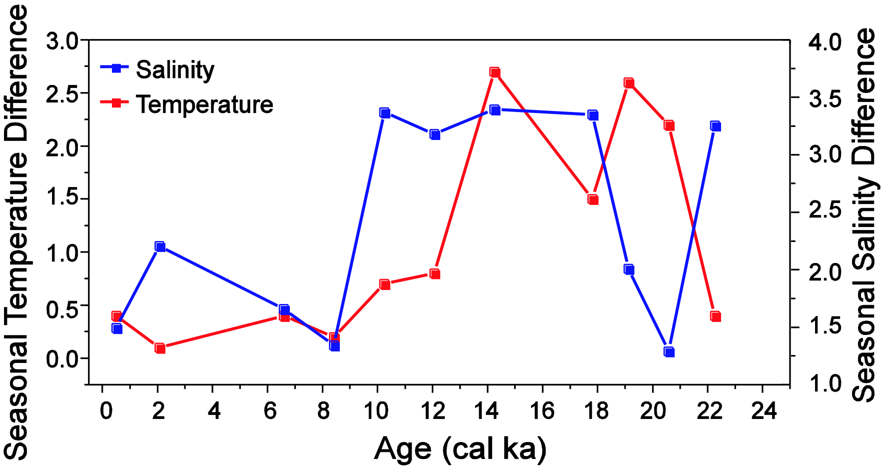

Figure 6. Seasonal temperature and salinity differences at the ODP Site 723A. Highest temperature and salinity differences are noticed during last glacial period.

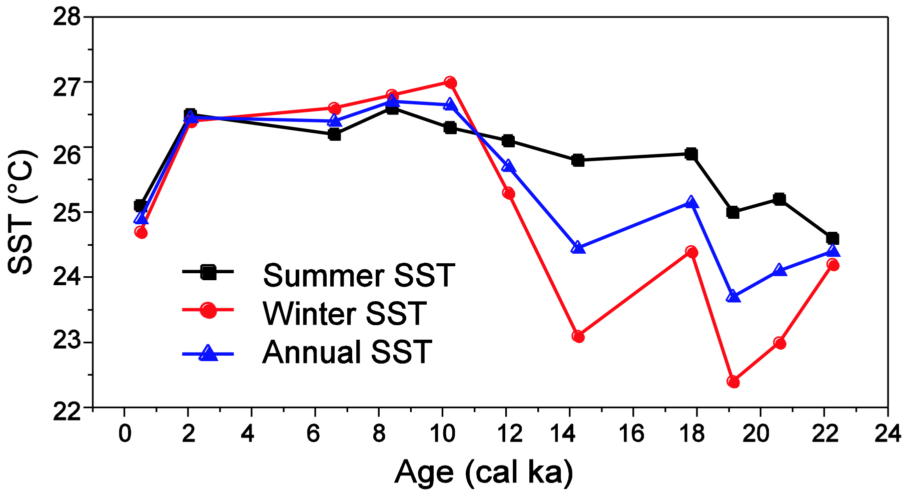

Figure 7. Fluctuations of summer, winter and annual SST at the ODP Site 723A.